

# The Tomographic Ionized-Carbon Mapping Experiment (TIME) CII Imaging Spectrometer

Z. Staniszewski · J. J. Bock · C. M. Bradford · J. Brevik · A. Cooray · Y. Gong · S. Hailey-Dunsheath · R. O’Brien · M. Santos · E. Shirokoff · M. Silva · M. Zemcov

Received: 21 August 2013 / Accepted: 4 February 2014 / Published online: 12 May 2014  
© Springer Science+Business Media New York 2014

**Abstract** The Tomographic Ionized-Carbon Mapping Experiment (TIME) and TIME-Pilot are proposed imaging spectrometers to measure reionization and large scale structure at redshifts 5–9. We seek to exploit the 158  $\mu\text{m}$  restframe emission of [CII], which becomes measurable at 200–300 GHz at reionization redshifts. Here we describe the scientific motivation, give an overview of the proposed instrument, and highlight key technological developments underway to enable these measurements.

**Keywords** Spectrometer · Reionization · Intensity · Mapping · TES · KID

## 1 Introduction

During the period between 200 Myr and one Gyr after the Big Bang ( $6 \lesssim z \lesssim 20$ ), the first baryonic objects collapsed in dark matter halos, ignited the first stars, and produced enough Lyman-continuum photons ( $h\nu > 13.6 \text{ eV}$ ) to reionize the surrounding hydrogen gas [1, 2]. The very first stars were likely metal free (containing only hydrogen and helium), short-lived, and ended in explosions that enriched the cosmos with the first heavy elements (e.g. [3]). Subsequent generations of stars then fully reionized the intergalactic medium (IGM). This epoch of reionization (EoR) is the first chapter in the history of galaxies and heavy elements, marked by the onset of the first generation of stars that represents a major transition in the history of the cosmos.

Detecting the individual primordial galaxies responsible for reionization is difficult as they are intrinsically low mass, low bolometric luminosity objects. Extremely deep

---

Z. Staniszewski (✉) · J. J. Bock · C. M. Bradford · J. Brevik · A. Cooray · Y. Gong · S. Hailey-Dunsheath · R. O’Brien · M. Santos · E. Shirokoff · M. Silva · M. Zemcov  
Department of Physics and Astronomy, California Institute of Technology,  
Pasadena, CA 91125, USA  
e-mail: zks@caltech.edu

imaging with the Hubble Space Telescope (HST) has begun to probe the very bright end of the UV luminosity functions at  $z > 6$  [4]. Our measurement uses an emerging technique that is sensitive to the integrated light produced by faint galaxies: spectral intensity mapping with 3-D spatial and spectral information to study EoR star formation rate density. We will use  $158\ \mu\text{m}$  line emission from ionized carbon (hereafter [CII]) to trace the light from star forming galaxies during the EoR. [CII] complements HI 21 cm line intensity mapping e.g. [5–7] that traces the neutral medium at  $z > 6$  (PAPER, MWA, LOFAR).

TIME and TIME-Pilot will be millimeter-wave imaging spectrometers that target the  $158\ \mu\text{m}$  ionized carbon fine-structure transition of [CII]. This spectral line is redshifted into millimeter-wave band which is accessible from high, dry sites. The [CII] measurement from TIME-Pilot traces the integrated star-formation rate density by measuring the aggregate [CII] intensity of proto-galaxies responsible for reionization.

## 2 Intensity Mapping

To study large-scale structure, the galaxy power spectrum is traditionally obtained by combining individual galaxy positions in 3D space. This approach cannot measure the total integrated quantities as the detections are limited to bright galaxies. In contrast, 2D total-intensity clustering measurements are sensitive to the spatial distribution of the whole galaxy population including sources below the point source detection threshold. However, 2D intensity studies in one or more broad spectral bands integrate over information along the line of sight with little or no distinguishing redshift information. This is particularly limiting for EoR studies because at most wavelengths the faint EoR galaxies represent a tiny contribution to the total light from all the galaxies along the line of sight.

3D intensity mapping combines imaging of spatial variations with spectral data, providing redshift information on the ensemble emission from galaxies. The approach is to select a single narrow spectral transition and then use an imaging spectrometer to measure a spatial-spectral data ‘cube’ in which intensity is mapped as a function of the sky position and frequency [8–11]. The frequency dimension corresponds to position along the line of sight through the frequency–redshift relation. Such a data cube can be used to measure the 3D power spectrum as a function of the spatial frequency  $k$ . The fluctuations due to large-scale structure are imprinted at low  $k$ , while the fluctuations at high  $k$  are simply due to the intrinsic variability in the number and brightness of galaxies in any given spatial box (i.e. Poisson noise). [CII] data cubes can be cross-correlated with HI 21 cm EoR data to trace the bubble size and ionization history of the IGM [11].

## 3 CII As a Tracer

While 21 cm EoR experiments target hydrogen in the IGM, [CII] measurements with TIME-Pilot target emission from the galaxies themselves. With a 11.3 eV ionization energy that is less than that of hydrogen (13.6 eV), carbon is easily ionized by diffuse starlight and is typically found in the singly ionized state in the interstellar medium

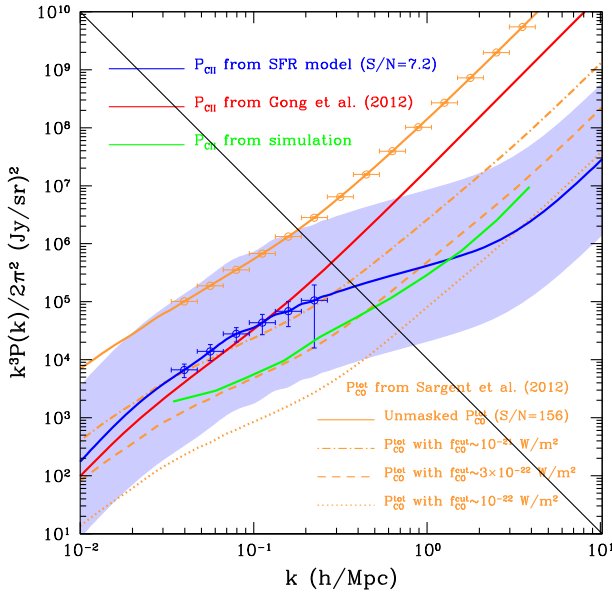


**Fig. 1** 3-D autocorrelation power spectra of EoR [CII] and intermediate- $z$  CO in the TIME-Pilot band. *Red, blue, and green curves* mark [CII] power from the ‘High,’ ‘SFR,’ and ‘Millennium’ estimates, respectively, described in the text. The *tan-colored lines* show power in CO: the *upper curve* includes all the CO-emitting galaxies, the *lower broken curves* show the power after masking to various depths (Color figure online)

(ISM). With a fine-structure level splitting of 91 K, [CII] is easily excited resulting in a line emission at  $157.7 \mu\text{m}$  through the  $^2P_{3/2} \rightarrow ^2P_{1/2}$  transition. [CII] is redshifted into the relatively-transparent  $1.2 \mu\text{m}$  atmospheric window (195–310GHz) for  $5 < z < 9$ , the target band for TIME-Pilot.

We have studied the prospects for mapping [CII] power spectrum with a wide-band imaging spectrometer, finding that the brightness variations of the [CII] line intensity can be used to map the underlying distribution of galaxies and dark matter [10–13]. To understand the detectability of [CII] from the EoR, we compare sensitivity estimates to three models for the signal. First, we compute the expected mean intensity of [CII] as a function of redshift and find a reasonable agreement when using one) the ‘high’ case model based on a first-principles gas physics excitation analysis, painted onto semianalytical galaxy formation models, and two) the ‘SFR’ case model based on an estimated high- $z$  star formation rate and a fixed [CII] to bolometric emission ratio of  $2 \times 10^{-3}$  [14]. As described in Gong et al. [11], the power spectrum then comes from partitioning this mean intensity into a galaxy luminosity function, and incorporating models for large-scale structure. We also compute three), a ‘Millennium’ case that applies a fixed [CII] to-bolometric-ratio of  $3 \times 10^{-3}$  to the De Lucia et al. [15] galaxy catalogs based on the Millennium simulation.

Figure 1 shows the sensitivity of our proposed instrument TIME-Pilot in 240 h on sky at the Caltech Submillimeter Observatory (CSO) compared to the two theoretical

[CII] power spectra. The dominant term is Poisson noise due to the random distribution of galaxies, but clustering becomes important on large physical angular scales. This large-scale clustering amplitude captures the total integrated [CII] line emission, which can be converted to the star-formation rate density through existing calibrations. The amplitude of the small-scale one-halo clustering term yields the typical halo mass scale of star-forming galaxies at  $z > 5$ . The latter is a crucial ingredient for models of galaxy formation and evolution since it establishes the halo mass scale in which gas cooled most efficiently and formed first proto-galaxies during reionization.

#### 4 The TIME Instruments

We propose building both the TIME and TIME-Pilot instruments. TIME-Pilot will use existing and proven technologies to obtain a first detection of the [CII] power spectrum in a small field. The full TIME experiment will be an order of magnitude more sensitive and relies on on-chip spectrometers now in development. It will survey many square degrees, providing high-SNR [CII] power spectra in several redshift bins suitable for cross-correlation with the coming HI datasets

TIME-Pilot, shown in Fig. 2, consists of 32-independent single-beam single-polarization spectrometers, each covering 195–295 GHz with 42 bolometers, making 1,334 bolometers in total. Each spectrometer uses a curved grating to both focus and diffract the radiation in parallel plate waveguide, providing a resolving power

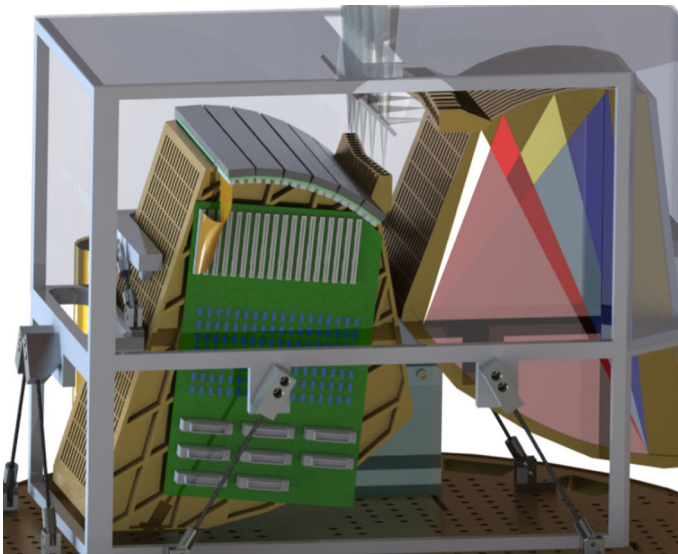


**Fig. 2** The TIME-Pilot instrument concept. Pictured are two spectrometer banks, each consisting of 16 single-polarization parallel-plate spectrometers. The *left* spectrometer bank depicts the location of linear arrays of TES detectors. We show one connection between a detector module and the first-stage SQUID board via flexible cable. The *right* spectrometer bank illustrates the diffraction grating's splitting of the *colors* toward different locations on the focal plane (Color figure online)

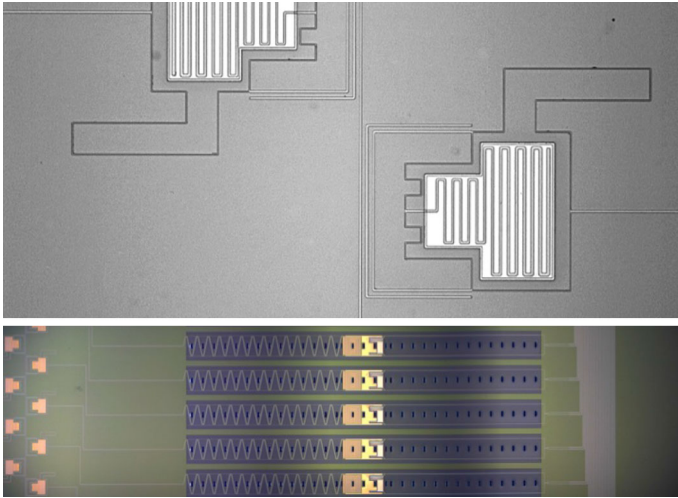


**Fig. 3** *Top* the resonant staple filter for one channel of the channelizer. Wide-band radiation travels down the center line in microstrip. Radiation is coupled inductively on to the staple and then from the staple on to lines that carry the power to the bolometer not shown off to the right. The out-of-phase power at the end of the staple should be zero, but is terminated in a lossy line. *Bottom* A subsection of the spectrometer. The resonant filters on the *left* hand side couple to the TES bolometers on the *right* (Color figure online)

R of 200. The bolometers each couple a  $\frac{\delta\nu}{\nu} = 1\%$ ,  $R = 100$  band, so that the detector sampling sets the channel width. The waveguide spectrometer is the same architecture as was used in the Z-Spec instrument [16], at the same frequencies but at higher resolving power than we require for TIME-Pilot. The detector sensitivity ( $\text{NEP} \sim 10^{-17} \text{ W Hz}^{-1/2}$ ) is readily obtained with a silicon-nitride leg-isolated TES bolometer using a titanium thermistor ( $T_c$  450 mK), and with a micro-mesh absorber ( $3 \times 3$  mm). The spectrometer output arc is approximated with six line segments, each will have either six (low frequency) or eight (high frequency) spectral channels.

Because we are particularly interested in measuring the low-k modes which are due to the underlying large-scale structure in the Universe, careful optimization is required. Some low-k information is provided by the line-of-sight (spectral) dimension given the large bandwidth, but we also aim to cover the low-k modes in a transverse direction, since the spectral dimension may have unique and challenging instrument/atmosphere systematics. Given the constrained number of spectrometers, we have found that the sensitivity to large scales is maximized by concentrating the spectrometers in a line on the sky, and scanning the instrument along this line. We thus define a  $156 \times 1$  beam ( $1.3 \text{ deg} \times 0.5 \text{ arcmin}$ ) field on the sky, which we cover by scanning the 1-D array of spectrometers ( $14' \times 0.6'$ ) back and forth along its length. Sensitivity calculations and simulations assume scanning at 4 arcmin/s, which is similar to the scanning speed of the Caltech Submillimeter Observatory (CSO). A faster scanning speed would be preferable.

For the full TIME experiment, we require of order 100 individual spectrometers covering a 2-D field, each providing R 300 or more (see Gong et al. [11]). This is a scope which is beyond the capability of an even compact grating spectrometers.

We are developing a new technology in which a complete single-beam spectrometer with integrated detector array is lithographically patterned in superconducting transmission line on a few square-cm piece of silicon. We are pursuing both TES and KID designs. See proceedings by [17, 18] for detailed simulations and demonstrations of prototype spectrometers.

In both implementations, the wide-band radiation is carried via transmission line microstrip toward a filter bank. For the TES version, we are patterning the antenna, transmission line, filter bank, and detector array on a single silicon wafer. The filter bank consists of half-wave resonant staples to couple the narrow-band signal off the transmission line, and another similar feature to couple on to the TES detector. Figure 3 shows both a subsection of the on-chip spectrometer and a detailed view of the resonant staple filter.

**Acknowledgments** We would like to thank the Keck Institute for Space Studies at Caltech and JPL for support of this concept study. Funding for R. O'Brien provided by the NASA Postdoctoral Program.

## References

1. G.D. Becker, W.L.W. Sargent, M. Rauch et al., *Astrophys. J.* **735**, 93 (2011)
2. D.N. Spergel, R. Bean, O. Doré et al., *Astrophys. J. Suppl.* **170**, 377–408 (2007)
3. V. Bromm, R.B. Larson, *Annu. Rev. Astron. Astrophys.* **42**, 79–118 (2004)
4. R.J. Bouwens, G.D. Illingworth, M. Franx et al., *Astrophys. J.* **686**, 230–250 (2008)
5. P. Madau, A. Meiksin, M.J. Rees, *Astrophys. J.* **475**, 429 (1997)
6. A. Loeb, M. Zaldarriaga, *Phys. Rev. Lett.* **92**(21), 211301 (2004)
7. N.Y. Gnedin, P.A. Shaver, *Astrophys. J.* **608**, 611–621 (2004)
8. T.-C. Chang, U.-L. Pen, K. Bandura, et al., *ArXiv e-prints*. (2010)
9. C.L. Carilli, *Astrophys. J. Lett.* **730**, L30 (2011)
10. E. Visbal, A. Loeb, *J. Cosmol. Astropart. Physics.* **11**, 016 (2010)
11. Y. Gong, A. Cooray, M. Silva et al., *Astrophys. J.* **745**, 49 (2012)
12. K. Basu, C. Hernández-Monteagudo, R.A. Sunyaev, *Astron. Astrophys.* **416**, 447–466 (2004)
13. Y. Gong, A. Cooray, M.B. Silva et al., *Astrophys. J. Lett.* **728**, L46 (2011)
14. R.C. Kennicutt Jr, *Annu. Rev. Astron. Astrophys.* **36**, 189–232 (1998)
15. G. De Lucia, J. Blaizot, *MNRAS.* **375**, 2–14 (2007)
16. C. M. Bradford, et al., *Society of Photo-Optical Instrumentation Engineers (SPIE) Conference Series*, vol. 5498, p. 257
17. E. Shirokoff, In this special issue LTD15 in *J. Low Temp. Phys.* (2013)
18. S. Hailey-Dunsheath, In this special issue LTD15 in *J. Low Temp. Phys.* (2013)